International Journal of Engineering & Technology, 7 (4.25) (2018) 173-180

International Journal of Engineering & Technology

Website: www.sciencepubco.com/index.php/IJET

Research paper

Flutter Analysis of High Aspect Ratio Wing of Sailplane Aircraft

Anis Khoirun Nisa*, Yorgi A.Ndaomanu, R.A. Sasongko, L. Gunawan, T. Mulyanto, Annisa Jusuf

Flight Physics Research Group, *Faculty of Mechanical and Aerospace Engineering,*
Institut Teknologi Bandung, Jl. Ganesha 10 Bandung 40132, Indonesia
**Corresponding author E-mail: aniskhoirunnisa@s.itb.ac.id*

Abstract

Sailplane aircraft that has high aspect ratio wing are often used in sports competitions in the sports gliding branch. One of the biggest aeroelastic problem of a plane with high aspect ratio wing is flutter. The occurence of flutter are caused by the combination of two or more normal modes. Flutter phenomenon that occurs in the sailplane aircraft generally are caused by the movement of aileron. To meet the certification purposes, flutter speed of aircraft should not occur within the safe limit of flight envelope. Certification that is used as a reference of design process is arranged by EASA at CS 22 that explain about the certification of sailplane aircraft. Flutter analysis was done using MSC NASTRAN/ PATRAN/ FLDS software. Analysis of the structure and aerodynamics plate is done by using the finite element method approach. The unsteady aerodynamic analysis was done using the Doublet-Lattice method, then flutter analysis was done using the PKNL method. Mode participation factor method is used to know the minimum mode shape that will appear when flutter occurs. Flutter speed is proportional to the magnitude of the wing stuctural stiffness. Beside that, aileron rod stiffness also give effects on flutter phenomenon. In this preliminary study, flutter analysis was done by varying aileron rod stiffness and general wing stiffness. Using the flutter analysis result, it can be seen that the differences on magnitude of aileron rod stiffness and general wing stiffness will have effect on the flutter speed magnitude.

Keywords: *MSC NASTRAN, PATRAN, FLDS, High Aspect Ratio Wing, Flutter, Mode Participation Factor, Control Surface, Aeroelastic.*

1. Introduction

The biggest aeroelastic problem of a sailplane aircraft which has a high aspect ratio wing is flutter. Flutter phenomenon occurs due to the involvement of three types of forces, which are elastic, inertia, and aerodynamics. Elastic force in the structure vibration phenomenon is caused by the component elasticity and deformability while inertia force is produced as consequence of the accelerations acting along wing span due to the existence of mass. Lastly, aerodynamic force is generated because there is flowing-air passing the lifting surfaces. [1] The combination of those forces could make the wing structure experience flutter. One cause of the occurrence of flutter in the flight envelope area is due to lack of stiffness on the overall wing or on the control surface.

One of many aspects which should be considered during the aircraft design process is that the aircraft must be ensured safe from flutter. Safe characteristic of flutter means that flutter will not occur within the aircraft flight envelope. One cause which is caused flutter in aircraft flight envelope is the lack of stiffness on the overall wing and/or control surface.

In the design process, it is required to do flutter analysis for the overall structure of the aircraft to determine whether the plane is safe from flutter or not. There are two ways that can be done to determine the aircraft speed that could generate flutter circumstance – ground test and calculation. To attain the aircraft certification, both ways must be done. Ground Vibration Test (GVT) is performed after the aircraft has been created, in order to measure eigenmodes with eigenfrequencies, generalized mass, and damping. In this preliminary study, flutter analysis is only undergone by using analytic model of half wing and GVT has not done. The analytical model is done by using finite element method approach. In order to pass certification, the analytical model must represent the real condition. For these needs, the model analysis should be analyzed by using more advance method, Doublet-Lattice method for subsonic. That method is used since the type of aircraft that is discussed in this study is subsonic regime aircraft. Unsteady aerodynamic model uses the finite element method to calculate aerodynamic forces on aerodynamic plate as used for structure model. On the flutter analysis, the eigenmodes amplitude is interpolated with the aerodynamic element, also called as generalized-airloads.

To prevent flutter, it is important to pay attention to the design on the control surface which the movement of these components can generate mentioned phenomenon. Therefore, the thing to do is to balance the control surface and ensure that the stiffness of the aileron rod actuator is safe/sufficient. The determination of rod actuator stiffness is important as design requirements of the actuator. In addition, to be able to withstand the aerodynamic load, it is expected that the control surface does not cause flutter. However, the most common type of flutter is caused by the aileron. [1] The relation between actuator stiffness – which connects aileron and wing – and the magnitude of flutter speed will be done in this study.

In real condition, the structure has damping force, but in this study, it will be ignored. Structural analysis is done by using MSC PATRAN software. Aerodynamic and flutter analysis uses MSC FLDS and MSC NASTRAN as those parameters calculation soft-

Copyright © 2018Authors. This is an open access article distributed under the Creative Commons Attribution License, which permits unrestricted use, distribution, and reproduction in any medium provided the original work is properly cited.

ware. The method used for flutter analysis is PKNL method (PK method with no looping).[4]
The output obtained from the flutter analysis is the velocity-damping curve and the velocity-frequency graph. However, the graph can not be used to determine any mode-shapes that have contributions in the occurrence of flutter. Moreover, there are minimum numbers of mode-shape hence wing experiences the flutter. Therefore, to know the combination of mode shape that will appear in flutter phenomenon by using the mode participation factor method (MPF). By knowing the mode-shape that participates in flutter, the designer can optimize the structure design that will be used. So, wing would have sufficient stiffness and flutter would not occur.

2. Method

2.1. Structural Modeling by Using Finite Element

In this study, half wing configuration and aileron are used to model the sailplane wing while flap is not modeled. It is assumed that flap structure is unity with the main skin. A half configuration wing and its aileron structure are modeled as separate components with the gap distance between them. Both components are connected by four hinges and one aileron rod. The data geometry of wing describe on the table below.

Table 1: Data Geometry

Data Geometry			
Span (tip to tip) (m)	**14.28**	**Twist angle (deg)**	**-3**
Root chord (m)	0.933	Aspect Ratio	17
Chord tip (m)	0.466	Area (m^2)	12
Dihedral (deg)	3	Airfoil	FX62K153
Outer taper ratio	0.5	Inner taper ratio	1

The ribs structure material is sandwiches composite and other parts are built by laminate composite. Each component has different lamina orientation angle. Between upper and lower skin, there is foam core to form the airfoil shape while manufacture process is conducted. Furthermore, the foam core is also applied to add the local bending (wrinkle) stiffness. In this study, foam core is not modeled as solid element, but thin shell element could be used to model with one condition: has the same mass when modeled as solid or thin shell element. This assumption could be applied since foam core has low contribution to the structure stiffness which causes generalized modes.
The skin and spar thickness are reduced from root to tip of the wing. Material properties which are used to model wing structure are listed in Table 1 The procedure to conduct structure analysis using the finite element method could be summarized in Fig.1 as flowchart form.

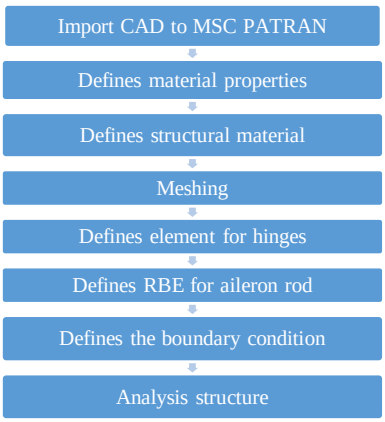

Fig. 1: The procedure to conduct structural analysis

Skins, foam core, spar and its webs, ribs, and aileron would be modeled in this study to construct wing structure parts. To simplify the model without neglected accuracy aspect, the spar-cap surface is formed by breaking the skin surface and giving the cut which is reflected spar-cap convenient thicknes. All parts are modeled as shell element because the thickness is smaller compared to the other two sides dimension. The finite element model with MSC PATRAN is use QUAD4 and TRIA3 shell element. Equivalence and verify must be done so that, mesh continues on the attached part.

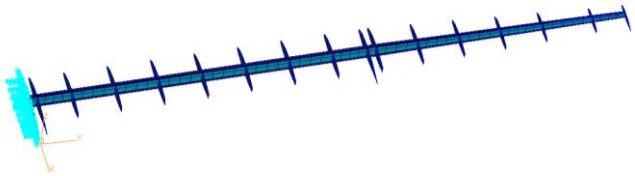

Fig.2: Ribs, spar-web, and spar-cap of the wing

Material properties of wing structure parts are defined as orthogonal 2D types of woven glass-fiber, and carbon-fiber. The orientation angle of each layer is determined based on the xy-plane (z axis shows the direction of thickness). Each component has different lamina direction. Therefore, axis definition becomes important step in order to get the right material properties of each parts.

Table 2: Material Properties

Part of Wing	**Material**	**Thickness/ Layer**	**Orientation (deg)**
Spar Web	Woven glass fiber (18 layers near the root section and decrease to 6 layers near the tip)	0.178 mm	0
Spar Cap	Carbon Fiber	The thickness of 2 cm on the taper of 1, and 1 cm on the taper of 0.5	0
Ribs	3 layers woven glass fiber + balsa wood + 3 layers woven glass fiber	Balsa wood of 2 cm	0
Skin	Woven glass fiber (5 layers near the root section and decreased to 1 layer near the tip)	0.178 mm	45

As mentioned earlier, aileron and wing are connected by using 4 hinges along the hinge line. Aileron hinge could be modeled on MSC PATRAN by using Multiple Point Constraint (MPC2) with RBAR element. This element defines a rigid bar with 6 degree of freedom at one end. To define RBAR, one independent node which has 6 degree of motion should be specified and the other nodes as dependent which may have less than 6 degree of freedom. [4] In this case, the nodes on wing-skin are defined as independent while the nodes in the aileron are dependent with 5 d.o.f which can rotate on the y-axis.
In addition, aileron rod is modeled as rotational spring by using spring element (CELAS1& PELAS). Rotational spring is allowed to rotate on the y-axis. Similar to RBAR, the spring element also connects two nodes, the nodes on the wing-skin and aileron. In this study, the spring element is defined to have various stiffness. For more details, rotational spring and RBAR model would be shown as follows. Two model which is used in this study are named as wing A (for a clean wing model) and B (for a wing and aileron model with high rotational spring stiffness).

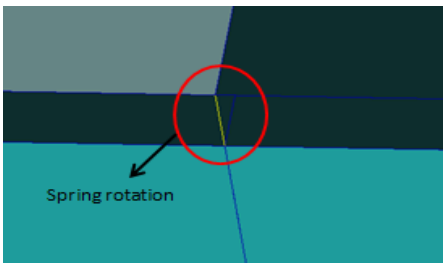

Fig. 3: Spring Rotation (CELAS1)

Fig. 4: RBAR in the hinge line

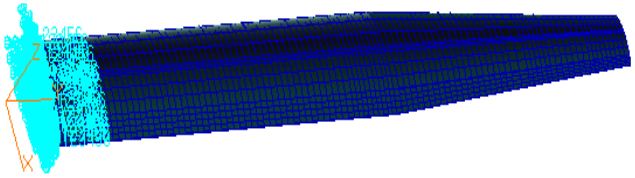

Fig. 5: Mesh and boundary condition of half wing

Wing model has fully constrained boundary condition at the root of the wing. The foundation is fixed across the surface of the ribs facing the fuselage located in the wings roots with the translational d.o.f is <0,0,0> and the rotation is <0,0,0>. Output data of structure analysis is required as input data for flutter analysis. The results of structure analysis are data of normal mode and natural frequency. Displacement along the wingspan of the normal mode is required to interpolate by using aerodynamic element.

2.2. Aerodynamic and Flutter Analysis

By using MSC FLDS software, the aerodynamic performance is modeled based on the Doublet-Lattice Method (DLM). The aerodynamic surface is assumed as plate. Plate-model of wing and aileron are created separately. So, there are two aero-plates on this model. Similar as structure analysis process, the aerodynamic analysis uses the finite element method. The plates are divided into small trapezoidal elements having at least two sides in the direction of the airflow and the positive x-axis. [3] If the structure coordinates which have been formed do not meet these requirements, new coordinates for the aerodynamic model shall be made. To model aircraft aerodynamic conditions, aerodynamic properties must be created. The aerodynamic properties input include density at sea level, reference length of wingspan, reference length of chord, and aerodynamic flow coordinate system. The aerodynamic condition along the full wing for xz-plane coordinates is symmetry, whereas for the coordinate xy-plane is not symmetric. The symmetry condition of the xy-plane coordinate is used if ground effect to the wing wants to be simulated. The reason of symmetrical aerodynamic condition is applied in the xz-plane coordinate since it is assumed that the wing tested in the wind tunnel is modeled as half-wing with fixed constraint at the root part on the xz-plane. The steps for modeling aerodynamics and flutter analysis by using MSC FLDS are summarized in Fig. 7.

To analyze flutter phenomenon, structure and aerodynamic elements must be interpolated or it is usual to be called aero-structure coupling or spline. Spline names in MSC FLDS must include the ID number of the spline. The recommended name for spline is with “name_ID” format. [5]

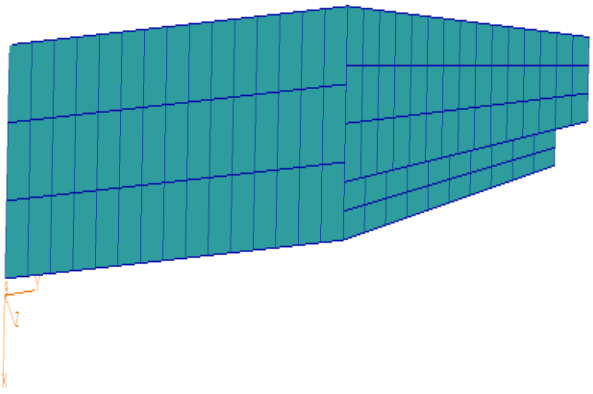

Fig. 6: Mesh and plate aerodynamic

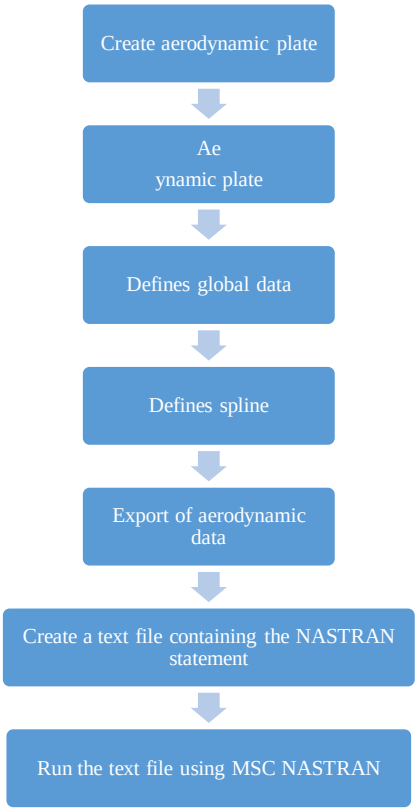

Fig. 7: The step of aerodynamic and flutter analysis

The spline is created by selecting a structure element that represents the displacement of normal modes along the wing and all the aerodynamic elements on the aero-plate. The definition process of a spline which is located between the aero-plate element and the structure element of the wing and the aileron is created separately.

By using Doublet-Lattice Method, each aerodynamic element has a control point located at the 75% chordwise station and spanwise center of the box. The lifting pressure that works across the surface of the element is concentrated in this control point. Normal and downwash boundary condition are located at each control points of the element.[3]

The last step in aerodynamic analysis using MSC FLDS is exporting aerodynamic data. For flutter analysis, the next step is creating a text file of bulk data that contains the NASTRAN statement in it. This statement is used to specify values for certain Executive System operational parameters [4]. Data which are required for flutter analysis are structural analysis output data, aerodynamic analysis output data, and aerodynamic parameters (MKAERO1) such as density ratio, Mach number, velocities, and reduced frequencies. These aerodynamic parameters are required for the needs of the FLUTTER statement input. Density ratio, Mach number, and velocities data are obtained from flight envelope of the sailplane aircraft.

The Nastran statement that is used to insert the external file is INCLUDE. The result of structure analysis which are contained in the bulk data are the grid data (GRID) and its structural elements (CQUAD4 and CTRIA3), material description structure (MAT8, PCOMP), displacement constraints (SPC1), and coordinate structure data (COORD2R). Meanwhile the information contained in the bulk data of aerodynamic analysis are global data (AERO), aerodynamic coordinates (CORD2R), aero surface plate (CAERO1, PAERO1), and spline (SPLINE4, AELIST). The aerodynamic parameters use the FLFACT statement for each parameter created.

After the bulk data of flutter analysis is created, then the file would be run in MSC NASTRAN to get flutter analysis output data. Natural frequency and damping for varied velocities of any normal mode are obtained as the results of flutter analysis.

3. Result

Mode-shape of each normal mode can be seen by taking a look at the result of displacement or strain energy along the wing. Flutter phenomenon can appear as consequence of combination of two or more normal modes with one normal mode must have a rotational part to induce additional unsteady lift as the flutter occurrence condition. [1] The normal mode with local deformation is considered to have no contribution to the formation of flutter phenomenon. The occurance of local deformation is caused by the nonuniform stiffness on some elements. In the normal mode, can appear multiple mode shape. To help knowing the dominant mode shape in the normal mode, it can be seen to the distribution of element strain energy. The difference of strain energy magnitude could be evaluated from the color spectrum of the element. The shape bending, torsion, inplane, and local deformation modes have different color spectrum distributions.

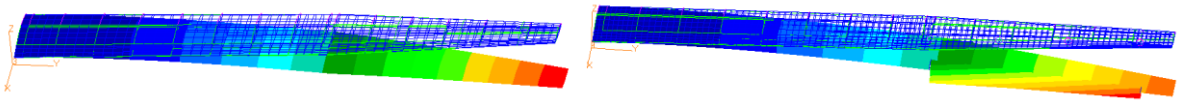

Fig. 8: Mode shape 1 Wing A, and Wing B

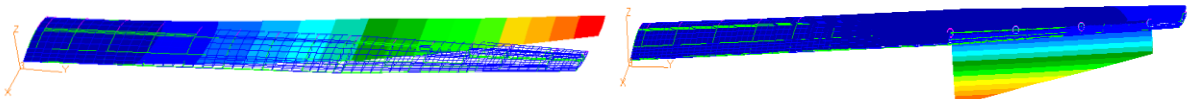

Fig. 9: Mode shape 2 Wing A, and Wing B

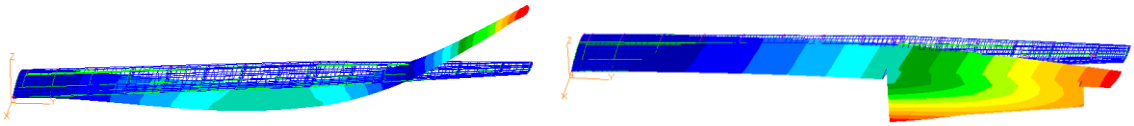

Fig. 10: Mode shape 3 Wing A, and Wing B

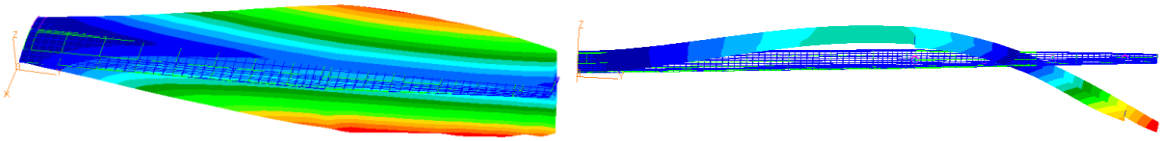

Fig. 11: Mode shape 4 Wing A, and Wing B

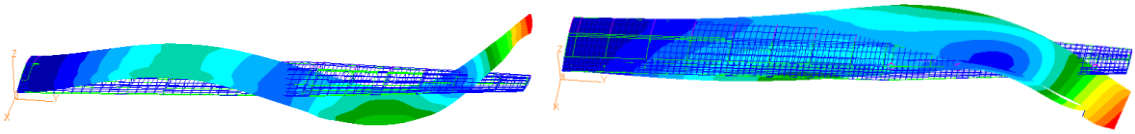

Fig. 12: Mode shape 5 Wing A, and Wing B

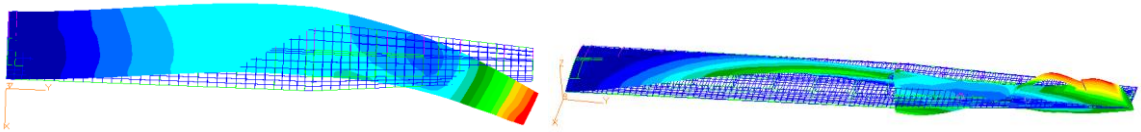

Fig. 13: Mode shape 6 Wing A, and Wing B

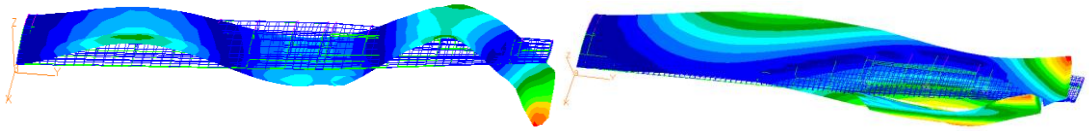

Fig. 14: Mode shape 7 Wing A, and Wing B

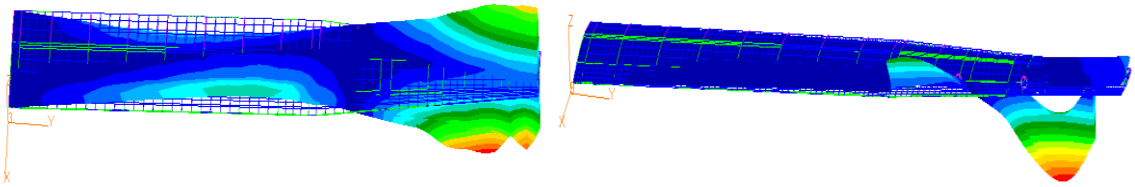

Fig. 15: Mode shape 8 Wing A, and Wing

Mode shape and natural frequencies for each mode are shown in the table below. Normal mode that is used for the analysis is only 8 normal modes. It happens because the mode shape in mode 9 only undergoes local deformation. So, it does not need to be included in the analysis

Table. 3: Normal modes of wing A

Mode Number	Natural Frequency (Hz)	Shape Mode
1	1.8734	1st bending
2	4.759	1st inplane
3	8.1952	2nd bending
4	17.238	1st torsion

5	18.858	3rd bending
6	19.758	2nd inplane
7	33.392	4th bending
8	35.228	2nd torsion

Table.4: Normal modes of wing B with high aileron rod stiffness

Mode Number	Natural Frequency (Hz)	Shape Mode
1	1.8561	1st bending + aileron deformation
2	3.716	Aileron deformation
3	4.7628	1st inplane + aileron deformation
4	8.1788	2nd bending
5	18.057	2nd inplane +aileron deformation
6	18.29	1st torsion + aileron deformation
7	19.854	3rd bending + aileron deformation
8	22.75	Aileron deformation

Table 5: Normal mode of wing B with low aileron rod stiffness

Mode Number	Natural Frequency (Hz)	Shape Mode
1	0.2022	Aileron deformation
2	1.763	1st bending + aileron deformation
3	4.331	1st inplane + aileron deformation
4	7.5487	2nd bending
5	16.412	1st torsion + aileron deformation
6	16.69	2nd inplane
7	18.19	3rd bending + aileron deformation
8	20.138	Aileron deformation

After obtaining the flutter analysis result, frequencies and damping of each normal mode are issued. Then both parameters should be analyzed to get the curve U-g (velocities - damping number) and the U-f (velocities - frequency).

3.1 Flutter Analysis Result

Flutter analysis was performed with the purpose to obtain the certification and for the design process. Flutter analysis using MSC NASTRAN gives an idea how big the speed that causes flutter. However, when the results are compared to the actual condition, error still occurs. It happens because the analysis model is not fully equal to the real wing geometry of the airplane. Moreover, there are several assumptions which make the results of calculation could not capture the phenomenon in real worlds.

Flutter phenomenon occurs because the structure is not damped so that the structure will continue to vibrate accompanied by aerodynamic forces that continue to work on the wing. Damping positive number means that the structure is not damped, and vice versa the other way around. The damped structure means that energy passing through the wing structure is transferred to the airflow. If the structure is not damped then the energy from the air flow is transferred to the structure so that the vibrations become more enlarged.

The results of the analysis in the form of graphs U- g and U-f can be seen in the graph below. The U-g and U-f graphs are plotted based on data obtained from each mach number variation. From the graph it can be seen that kind of mode shape and speed of flutter phenomenon occurs. Mode Participation Factor (MPF) must be done to find any participating mode shape that will appear at the time of flutter. Estimates of the minimum normal mode that will appear at the flutter phenomenon can be seen from the flutter eigenvector. Eigenvector data of a particular velocity that have positive damping can be extracted by adding a minus sign in front of the speed at FLFACT entry. Two sets of eigenvectors will be generated, one of which is in modal coordinates (the eigenvector generated as part of the eigenanalysis capital complex) and the other in physical coordinates (eigenvector that results when the eigenvector is expanded to the physical coordinates using the normal eigenvectors). [3] The eigenvector data consists of real and imaginary numbers. Furthermore, to check the combination of some normal mode that suspect will appear in flutter phenomenon by add SET statement (select mode to be analyzed) and MODESELECT in bulk data entry. Then, MSC NASTRAN will analyze these modes only. If from the analysis of these modes produce positive damping, then it can be stated that flutter may occur. To knowing dominant normal mode that will appear in the flutter, it can use mode participation factor to give guessing. Otherwise, if some mode is analyzed, do not produce positive damping then combination of some mode will not cause flutter.

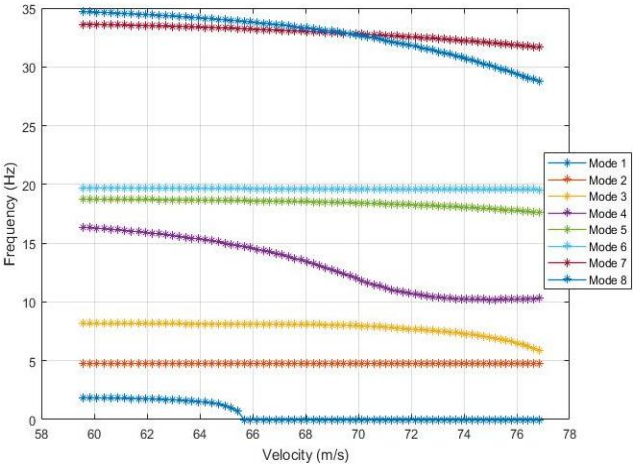

Fig.16: Graph U-f of wing A

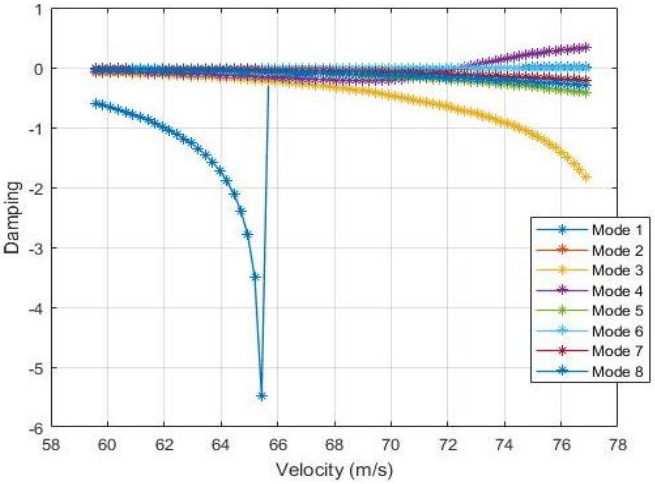

Fig.17: Graph U-g of wing A

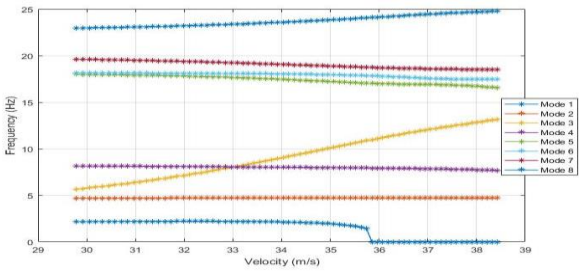

Fig.18: Graph U-f of wing B

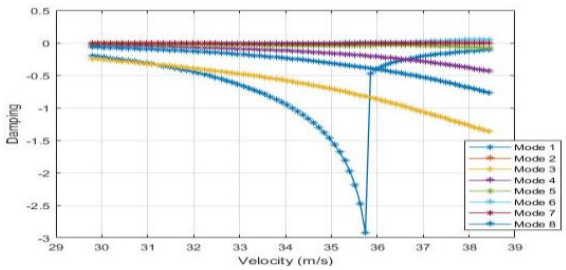

Fig.19: Graph U-g of wing B

Fig. 16 and 17 are graphs of U-f and U-g at Mach 0.5 to model clean wing (Wing B). Fig.16 shows the variation in the frequency

of the velocity on the wing B. From the graph it can be seen several modes of increasing frequency as the speed changes up to the speed of the flutter. Fig.17 shows the variation of the magnitude of the damping ratio of the speed to wing B. From this graph can be seen that the mode 5 (1st torsion) has a positive damping (undamped) at a speed of 186.67 m / s. To know the combination between mode 5 and other modes which causes flutter, it is necessary to do participation factor mode with the result shown in Fig. 20.

While in Fig. 18 and 19 are graphs U-f and U-g at Mach number 0.3 for the wing and aileron models with high spring rotation stiffness. From the graph, it can be concluded that the wing will have a flutter at a speed of 108.88 m / s. In Fig.19 it can be seen that the mode having positive damping is the mode 6 (1st torsion + aileron deformation). For these two models, 1st torsion mode shape has contributed to the occurrence of flutter.

To simplify the variation of combinations between modes the following the MPF methods can be performed:

Percentage = √ ((R ^ 2 + I ^ 2))

With,

R = real eigenvector

I = imaginary eigenvector

The way above can be done to guess the normal mode that causes flutter phenomenon. The combination of normal modes is done by continuing to eliminate normal modes with small percentage into the combination. If the combination of some normal mode with the bigest percentage has not produced a positive damping, then the combination of previous modes that produce positive damping is the dominant normal mode that appear in the flutter phenomenon. If some normal mode of MPF result has not happened all or one of its modes hence flutter phenomenon will not happen.

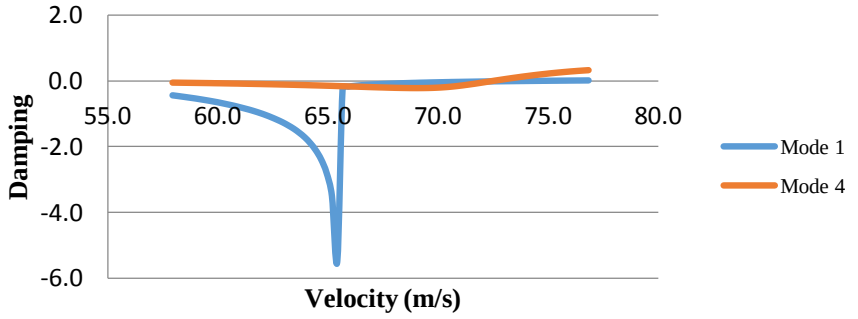

Fig. 20: Mode Participation Factor clean wing model

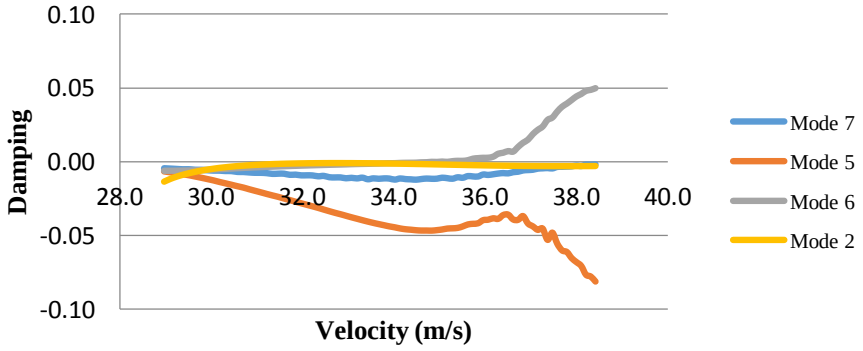

Fig. 21: Mode Participation Factor wing and aileron model

The graph at Fig.20 shows that the mode 5 and 6 are the minimum modes that cause flutter phenomenon on the clean wing model. Before doing a combination of both modes above, the combination between the other mode is done. Mode 5 on this model is 1st torsion while mode 6 is 4th bending. And for Fig.21, the graph shows that the mode 2, 5, 6, 7 are the minimum modes that causes flutter phenomenon on the wing and aileron model. The shape of the modes are aileron deformation, third bending, first torsion, second torsion.

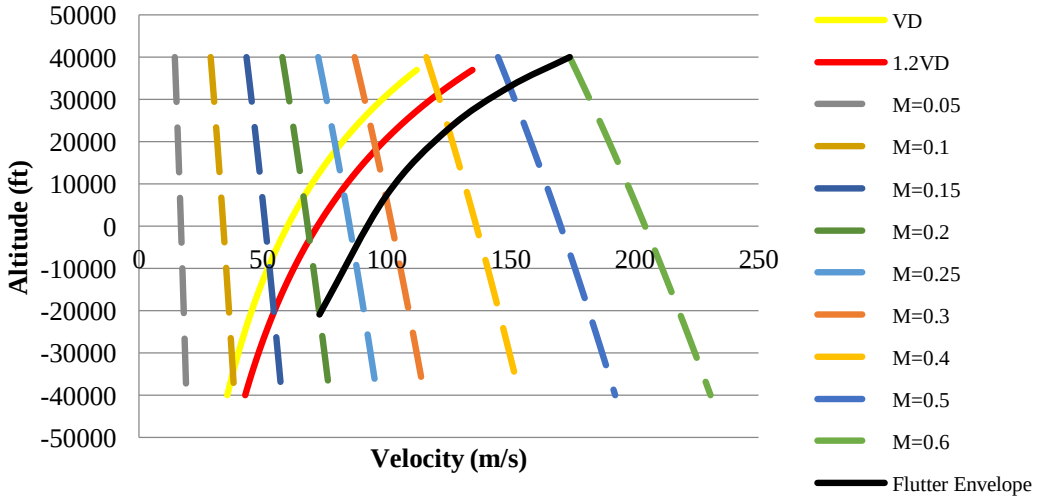

Fig. 22: Flutter envelope of composite clean wing model

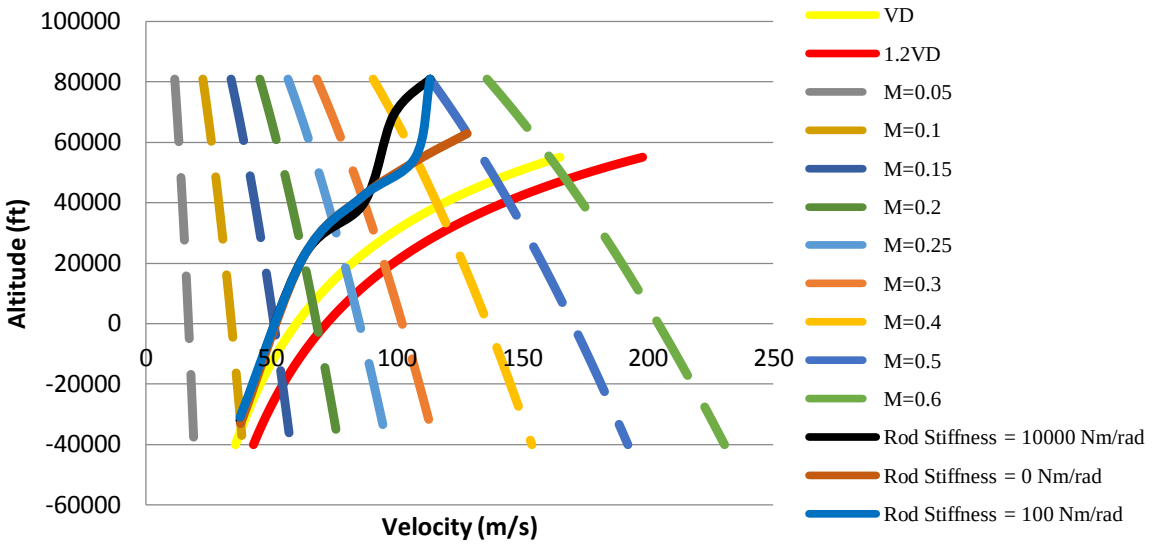

Fig. 23: Flutter envelope composite wing and aileron model

From Fig. 22, it can be seen that the clean wing model has a flutter outside the safe envelope limit. Therefore it can be concluded that this model is safe from flutter. The flutter speed at sea level is 93.226 m/s while the safe limit speed of flutter is 72 m/s. On Fig. 23 is shown that wing and aileron model not save from flutter. All variation stiffness of aileron rod model has flutter line within the safe boundary of the flight envelope. This occurence of flutter may be due to a lack of siffness structure so that the stiffness of aileron rod will not give effect to flutter at all. Based on mpf result, mode shape that appear in low aileron rod stiffness model is aileron deformation, 1st torsion, 2nd inplane, and 3rd bending. Based on this result, the effect of aileron rod stiffness to flutter speed cannot be seen. The flutter occurs due to a less stiff of structure, and not because of aileron deformation.

As a comparison, to prove that the magnitude of aileron rod stiffness will give effect to occurence of flutter, then structure modelling will be done again with same geometry but has different properties. Material properties for this new model is alumunium 2024 T-3. The general wing mass of this model is same as composite model (60 kg), but has different stiffness. The volume of the wing is changed until the two model has the same mass. Even so mass of aileron is different between this two model. By doing the same modelling step as explain above, flutter envelope of new model with alumunium material describe Fig. 24. Based on that figure, wing with low aileron rod stiffness model will experience flutter at low Mach number. Flutter will occur at Mach 0.1, and positif damping will appear at mode shape aileron deformation. The flutter speed of this model is 28.97 m/s. And for wing with high aileron rod stiffness model is safe from flutter occurence. The flutter line beyond safe limit of flight envelope. The flutter speed of this model is 112.12 m/s and at Mach number 0.3.

4. Conclusions

From this study, it can be seen that wing A and wing B with high aileron rod stiffness model have the same first normal mode natural frequency. It proves that the aileron rod can represent the node connection on the clean wing model. Natural frequency of wing B with low aileron rod stiffness is very small. It is in accordance with the lack of stiffness in the hinge line.

Mode shape that appear when flutter occur is different among wing A model and wing B model. Flutter at wing A model has fewer mode shape that appear than wing B model. The appearence of mode shape when flutter occur, also determined by the stiffness of the general wing. If wing has high stiffness then only few mode shape that appear, so vice versa.

Flutter speed of different aileron rod stiffness model with composite material have no difference between a model and another model. Flutter phenomenon occur because the lack of wing stiffness or aileron stiffness and not because of the aileron movement. From this modelling the effect of aileron rod to the flutter speed cannot be seen.

Therefore other modelling is done by changing the structure stiffness but the mass remains. The structure stiffness is changed from previous model because the previous model was thought to have low stiffness so that flutter speed still the same although the aileron rod stiffness has changed.

The result of wing B model with alumunium 2024 T-3 properties can be seen on Fig. 24. According to the analysis of wing with low aileron rod stiffness model, flutter will occur at Mach number 0.1, while wing with high aileron stiffness model will experience flutter at Mach number 0.3. It can be concluded that the smaller aileron rod stiffness, then flutter will occur in lower speed and Mach number.

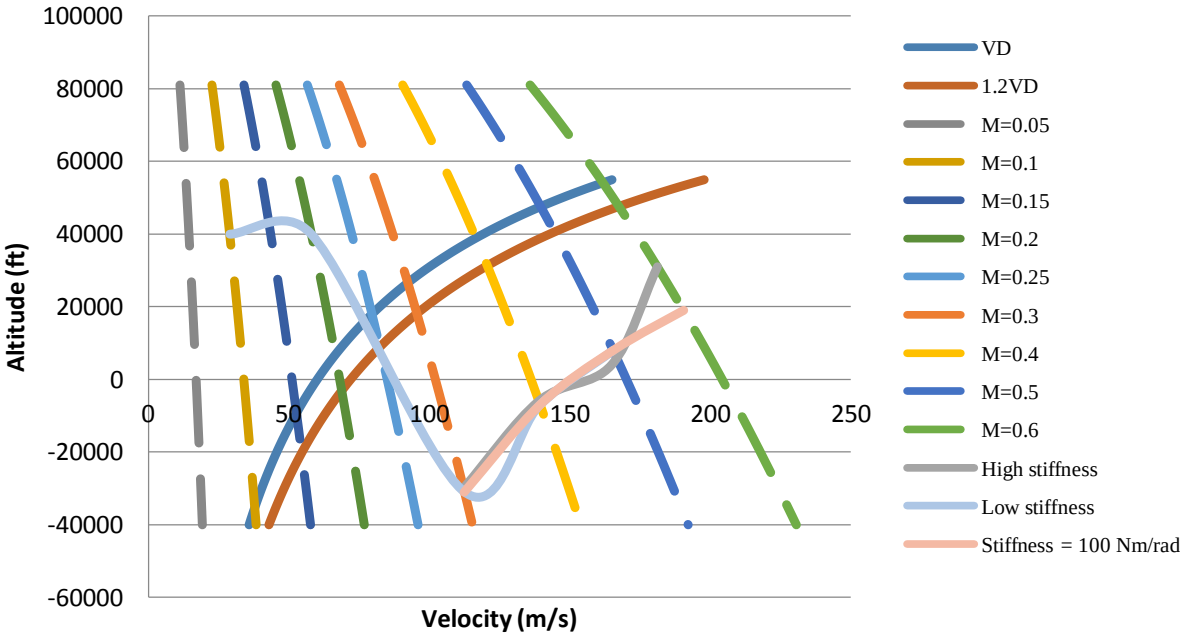

Fig. 24: Flutter envelope wing and aileron model alumunium 2024 T-3

References

[1] Pajno V. Sailplane Design. (2010). Roma: la Pubbliprint Service

[2] Zwaan RJ. Aeroelasticity of Aircraft. (1990). TU Delft

[3] MSC Software. MSC. Nastran Version 68 Aeroelastic Analysis User's Guide. Retrieved from www.mscsoftware.com

[4] MSC Software. (2011).MD Nastran 2011 & MSC Nastran 2011 Quick Reference Guide. Retrieved from www.mscsoftware.com

[5] MSC Software. (2006). MSC. FlightLoads and Dynamics User's Guide Version 2006. Retrieved from www.mscsoftware.com

[6] Hodges DH and Pierce GA. (2011). Introduction to Structural Dynamic and Aeroelasticity. Cambridge: Cambridge University Press

[7] Clark R, Cox D, Curtiss HC, Edwards JW, Hall KC, Peters DA, Scanlan R, Simiu E, Sisto F, Strganac TW. (2005). A Modern Course in Aeroelasticity.New York: Kluwer Academic Publishers

[8] Wright JR and Cooper JE. Introduction to Aircraft Aeroelasticity and Loads. England: John Wiley &Sons Ltd

[9] European Aviation Safety Agency. (2008). Certification Specifications for Sailplanes and Powered Sailplanes CS-22. Retrieved from www.easa.europa.eu